Engineering Research Express

PAPER

Microstructure and anti-corrosion properties of spray pyrolyzed Ni-doped ZnO thin films for multifunctional surface protection applications

Engineering Research Express

PAPER

Microstructure and anti-corrosion properties of spray pyrolyzed Ni-doped ZnO thin films for multifunctional surface protection applications

RECEIVED
15 January 2021

REVISED
1 April 2021

ACCEPTED FOR PUBLICATION
9 April 2021

PUBLISHED
26 April 2021

Victor Adewale Owoeye[1], **Emmanuel Ajenifuja**[2,3,4], **Abiodun Eyitayo Adeoye**[5], **Ayodeji Olalekan Salau**[6], **Adedeji Tomide Akindadelo**[7], **David A Pelemo**[2] **and Abimbola Patricia Idowu Popoola**[3]

[1] Department of Physical and Chemical Sciences, Elizade University, Ilara-Mokin, Nigeria
[2] Centre for Energy Research and Development, Obafemi Awolowo University, Ile Ife, Nigeria
[3] Department of Chemical, Metallurgical and Materials Engineering, Tshwane University of Technology, Pretoria, South Africa
[4] Center for Energy and Electric Power, Tshwane University of Technology, Pretoria, South Africa
[5] Department of Physical Sciences, First Technical University, Ibadan, Nigeria
[6] Department of Electrical/ Electronics and Computer Engineering, Afe Babalola University, Ado-Ekiti, Nigeria
[7] Department of Basic Sciences, Babcock University, Ilishan Remo, Nigeria

E-mail: ayodejisalau98@gmail.com

Keywords: 316 stainless steel, corrosion, pyrolysis, grain size, SEM, EDX

Abstract

The microstructures, electrochemical, and hardness properties of deposited Ni-doped ZnO thin films on ultrasonically cleaned 316L stainless steel (316L ST) employing a low-cost chemical spray pyrolysis technique (CSPT) was examined in this work. The films were prepared at various concentrations using commercially available purity zinc acetate and nickel acetate as the precursor sources. The result of x-ray diffractometry (XRD) showed that the films have polycrystalline structure with all the films consisting of single phase ZnO hexagonal wurtzite structure. Scanning electron microscopy (SEM) result affirmed that the coated films adhered to the substrates and equally spread through the substrate surfaces. The surface microstructure of the 316L ST improves with Ni content. The corrosion resistance of the 316L ST was observed to improve with the coated films. Hardness value of the uncoated 316L ST was observed to increase from 139.15 HV to 233.03 HV of coated S3 (9% nickel acetate (0.2 M) and 91% zinc acetate (0.2 M)).

1. Introduction

Metals and alloys fail when their surfaces are exposed to corrosive environment. Covering the material's surface with thin films can delay and thus prevent fast corrosion. Considering available literature, few reports exist on doping of Ni with ZnO to improve on corrosion resistance and wear properties of stainless steel. This study therefore intends to evaluate the role of the presence of Ni in Ni-doped ZnO on surface morphology, corrosion resistance and hardness properties of 316L stainless steel using chemical spray pyrolysis technique (CSPT) for multifunctional surface protection applications. Stainless steel has diverse applications mostly in the chemical and car manufacturing industry . Preventing this material from industrial accidents attributed to corrosion is of great concern.

Surface modification of engineering materials is often resourceful than working on the entire bulk properties as this is significant because every mechanical activity takes place at the surface of engineering materials [1–3]. Various methods such as nitriding, carburizing, induction hardening, laser induction and internal oxidation have been used to improve surface properties of materials [4–8]. Surface protection through the organic coating system is the most dynamic method recently used to protect different kinds of atmospherically exposed steels against corrosion [9, 10]. The nature of steel surface is greatly affected by the effectiveness of its protective coatings. Studies have shown that coatings on smooth surfaces have lesser corrosion resistance and weaker adhesion than coatings applied on grit blasted surfaces [11]. Metals such as Mild steel and AE44 magnesium alloy

which form a passive layer on their surface upon exposure to the corrosive media have high corrosion resistance with a decrease in surface roughness than those with no passive film [12]. Reports also have it that an increase in the surface roughness of stainless steel and some other alloys increases the corrosion resistance [13, 14]. Authors in [15] showed that an increase in the surface roughness decreases the pitting potential in 304L stainless steel in saline environment. The stability of coating-substrate interface is a function of the interfacial adhesion forces and electrochemical properties of the region [10]. McBain and Hopkins [16] gave the importance of surface roughness on adhesion. In their study, they considered surface roughness as a major contribution to adhesion by mechanical interlocking. Brockman [17] also suggested that bond durability is determined by the surface roughness, as mechanical interlocking continues to operate even when chemical bonds fail. Authors in [18] suggested that interfacial stability of protective coatings in corrosive environments can be influenced by mechanical interlocking. Machining is also said to give surfaces protection where protective coating provides long lifetime by optimal selection of cutting parameters.

Corrosion in metals and alloys pose a major challenge as corrosion results to the damage of various metallic components in industrial plants [19, 20]. Corrosion of engineering materials is a function of its applicability. Steel is corroded when electrochemical process is instigated by certain electrolytic environments in the vicinity of the steel chamber. The constituent elements of stainless steel determine the level to which it will resist corrosion in corrosive environments [21]. Huge amounts are spent globally to maintain this epileptic situation. Among the types of steels, austenitic stainless steels are mostly used in large proportion because of their high level of weldability, high melting point and good resistance to corrosion. Austenitic stainless steels such as 316L, 316, 304L, 304, and AISI are used in the fabrication industry for the manufacture of various equipment [22]. The level of industrial action and the environment to which stainless steels are exposed results in their failure; thus in some studies, this is considered as a technical problem. Few studies have analyzed details of stainless steel with the aim of intensifying efforts to limit this challenge [23, 24]. As part of efforts to limit corrosion of stainless steels in various applications, different studies have been carried out on corrosion of stainless steels in some acidic and saline environments [25–27].

However, Ni-based alloys have been reported to have thermal and microstructural stability which improves mechanically through alloying with some transition metals like titanium and chromium [19, 28]. Reports have it that transition metals e.g., titanium, vanadium, chromium, nickel, and zinc enhance wear resistance, corrosion resistance as well as increase the hardness of materials [29–32]. Nickel-based alloys are used in various industrial applications such as petrochemicals, nuclear, pharmaceutical, glass and auto-mobile owing to its high resistance to wear and corrosion [33–35].

Coating is said to be an art that offers protection to material surfaces through the protection of some specific parts of materials from mechanical stress and corrosive environments in different fields ranging from automotive, marine, and aerospace industry [36]. The considerable wide band gap of n-type semiconductor ZnO makes it outstanding in all rounds of applications mostly in optoelectronics application. The anticorrosion behavior of nanostructured ZnO thin films on 304L stainless steel was investigated by Muhamed *et al* [37]. The authors observed thatthe anticorrosion behavior of 304L steel improved with coated ZnO thin films. The study was carried out in saline environment. In addition, the authors did not consider the effects of acidic environments . Precipitation deposition technique was employed in the study . This method may not give the best anticorrosion properties of stainless steel because with the help of spray pyrolysis technique, the substrate must have been pre-heated. Pre-heating the substrate will not only enhance adhesion of the films to the substrate but will also enhance corrosion resistance and aid uniform deposition. In Ibrahim *et al* [38], nanocomposite ZnO-NiO particles were coated on mild steel by sol-gel method for anti-corrosion applications in saline environments. The corrosion resistance of the coated ZnO-NiO nanocomposite was reported to improve greatly compared to the uncoated mild steel using electrochemical impedance spectroscopy analysis which showed little changes.

The study carried out by Matero *et al* [39] involved the deposition of multilayers Al-TiO_2 films on ST substrate using atomic layer deposition reactor technique. It was observed that TiO_2 does not give a good protection on stainless steel in both NaCl and HCl environments. However, it was found that multilayers Al_2O_3-TiO_2 films give a better protection on the substrate in both environments. A similar research was carried out by Fusco *et al* [40]. In their study, Al_2O_3 and TiO_2 thin films were also deposited using the same deposition technique in NaCl environment. The coated samples were observed to show increase in polarization resistance with 12 MW-cm^2 as measured by impedance spectroscopy over the uncoated copper. The work of Mohamed *et al* [41] involved the deposition of ZrO_2, TiO_2-SiO_2 and Al_2O_3 films coated on 316L stainless steel in both acidic and basic media using sol-gel technique. The authors reported that the films improved the lifetime of 316L ST and blocked the layers against corrosive media. The corrosion rate of the coatings was observed to be 10 times lesser than that of the uncoated 316L ST. The polarization resistance of the coatings was observed to be much higher than that of the uncoated copper. The polarization curves of TiO_2-SiO_2 and Al_2O_3 were found to be more active than ZrO_2.

Table 1. Mixing ratio of the Ni-doped ZnO precursors.

Sample Name	Reacting solution (percentage & Concentration)
S0	316L Stainless steel (Control)
S1	3% nickel acetate (0.2 M) & 97% zinc acetate (0.2 M)
S2	6% nickel acetate (0.2 M) & 94% zinc acetate (0.2 M)
S3	9% nickel acetate (0.2 M) & 91% zinc acetate (0.2 M)

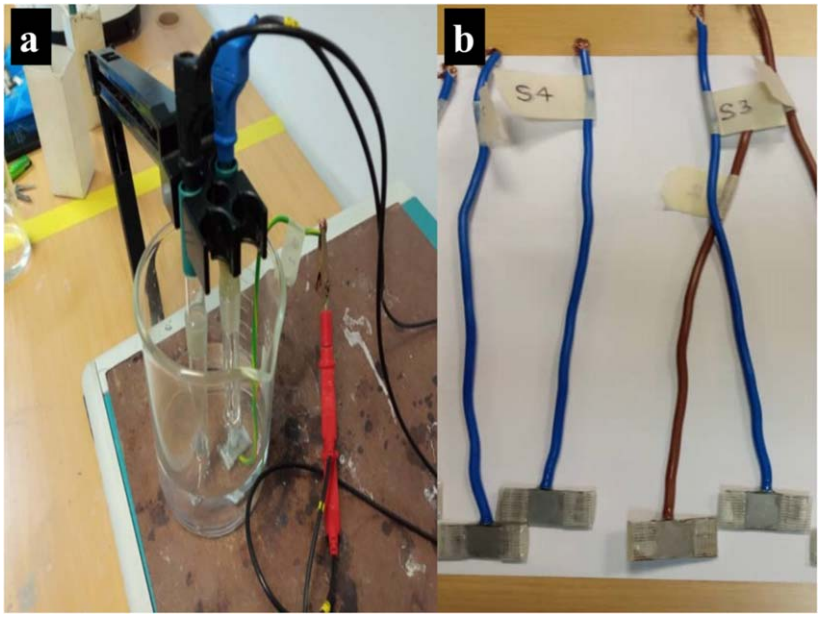

Figure 1. (a) Corrosion electrochemical experiment setup (b) some characterized samples.

Materials are nanostructured by either top-down or bottom-up approach, thin films method of nano structuring materials is a typical example of bottom-up approach. Thin film is a layer of material that can be found in the range of nanometer to several micrometers in thickness which has a thin layer with distinct properties from bulk materials. Studies on thin films are of great interest because of the uniqueness in their properties such as the surface to volume ratio compared to bulk nanostructured materials, their structure, morphology, and physical features are quite different from bulk materials, their microstructures because of growth process which is related to their physical properties are quite excellent than bulk nanostructured materials [42]. Spray pyrolysis technique (SPT) is one of the growing techniques used for thin films deposition. The usefulness of SPT over many deposition techniques were reported in [43–45].

2. Materials and methods

2.1. Materials

The substrate material used in this work is a commercially available type 316L austenitic stainless steel of average nominal composition; 44.5%Fe, 10.5%Cr, 5.8%Ni, 16.6%O, 13.5%Si, 6.4%Al, 1.3%Mg, 0.9%K, 0.2%Ca, and 0.2%Ti. The material is flat with a thickness of 0.16 cm (1.6 mm). It was machined to sample size dimension of 2.85 cm by 1.24 cm. Commercially available purity zinc acetate ($Zn(CH_3COO)_2.2H_2O$) and nickel acetate ($Ni(CH_3COO)_2.3H_2O$) were used as source precursors and both were dissolved in distil water.

2.2. Thin films preparation

Various samples of Ni-doped ZnO films were prepared on ultrasonically cleaned 316L austenitic stainless steel (2.85 cm $\times$ 1.24 cm $\times$ 1.6 cm) by preparing different molar concentrations of Nickel acetate and zinc acetate precursors in distilled water, respectively. The methods used for solution preparation and molarity calculation were reported in our previous work [43]. Table 1 summarizes the mixing ratio of the Ni-doped ZnO precursors.

These precursor solutions were briskly stirred for some minutes before spraying onto preheated cleaned 316L ST substrates maintained at (350 $\pm$ 5) °C. Meanwhile, to achieve good quality thin films, all deposition parameters were optimized [43]. The chemical reaction to obtain the desired film is presented in Equation (1)

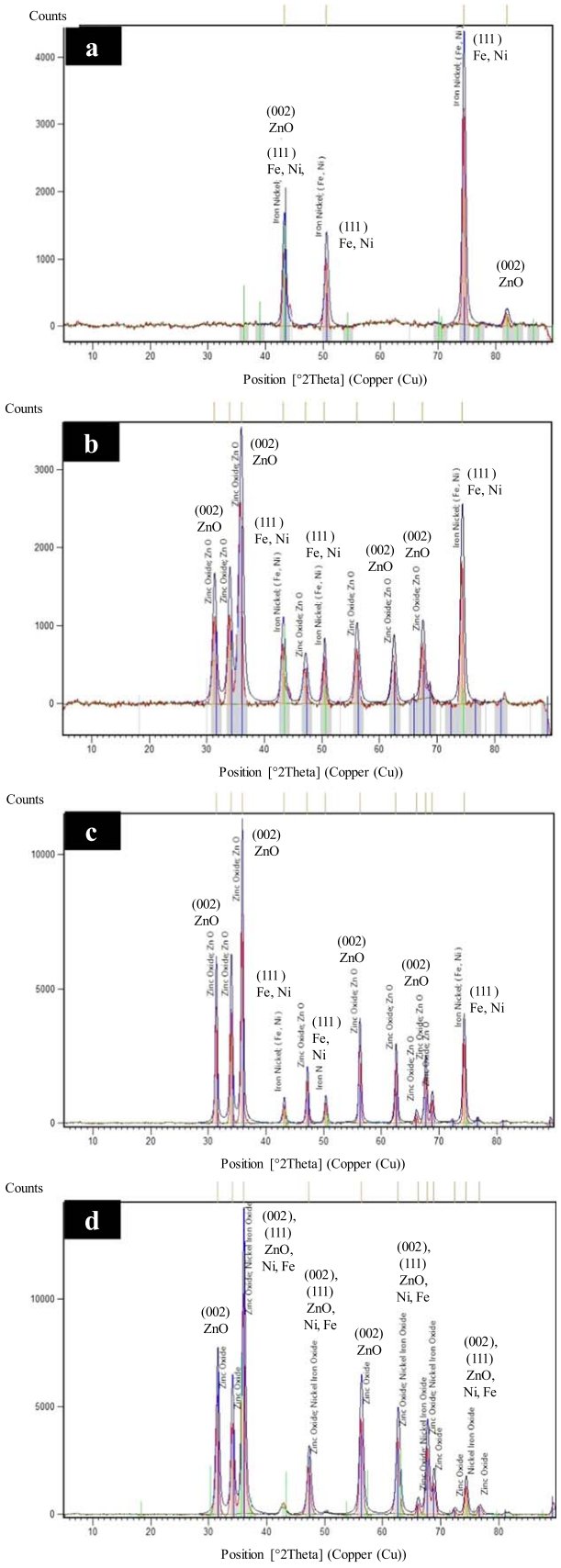

Figure 2. (a). XRD spectra of S0. (b). XRD spectra of S1. (c). XRD spectra of S2. (d). XRD spectra of S3.

$$Ni(CH_3COO)_2.3H_20_{(aq)} + Zn(CH_3COO)_2.2H_20_{(aq)} \xrightarrow{\Delta} NiZn0_{(l)} + 5CO_{2_{(g)}} + 3CH_{4_{(g)}} + 3H_{2_{(g)}} + 2H_20_{(g)} \quad (1)$$

2.3. Characterization

The prepared samples were characterized using SEM with attached EDX (JOEL JSM-7600F FE-SEM) and XRD (PW1710 Philips) with Kα Cu radiation at 40 mA and 40 kV to examine the morphology, elemental composition, and microstructures of the samples, respectively. PANalyticalX'Pert High Score software was used to analyze the diffractometry data.

2.4. Electrochemical measurement

The sample size dimension of 2.85 cm by 1.24 cm with diameter 0.16 cm with an exposed surface of 2 cm^2 was used for the electrochemical experiment, while the other side of the sample was coated with an epoxy insulating material to prevent corrosion attack on the surface where no measurement was carried out. A solution of H_2SO_4 was employed as the corrosive environment with concentration of 0.1 M, silver chloride (Ag/AgCl) was employed as reference electrode, platinum was applied as the counter electrode while the samples serve as the working electrode. The electrochemical properties of the samples were analyzed using the Autolab potentiostat galvanostat (PGSTAT) method, and the corrosion potential was measured using a potentiostat while the corrosion current was measured using a gavanostat. The polarization curves for the samples were obtained by plotting the graph of corrosion potential against corrosion current. In Figure 1 we show the picture of the corrosion test arrangement of some of the samples.

2.5. Microhardness testing

The effect of Ni-doped ZnO thin films on the hardness properties of 316L ST was evaluated using Tensometer TypeW microhardness tester incorporated with Vickers hardness (HV) test model Fm-8033 at Tshwane University of Technology, Pretoria, South Africa. A diamond tip was applied to indent on the surface of the samples with a maximum constant loading rate of $P\mathrm{max} = 100$ gf. To ensure accuracy, the indentation was carried out at different areas of the sample's surfaces and the average values were recorded using the Tensometer TypeW microhardness tester in HV for each of the samples. To evaluate the influence of Ni-doped ZnO thin films on 316L ST, the hardness value of the substrate was also evaluated separately. Since Berkovich indenter was employed, permanent imprints indicated by the arrows in Figure 6 were observed after load removal. These permanent imprints are due to elastic-plastic deformation of the films [46]. The hardness values of HV were determined by using the Tensometer TypeW microhardness tester by using the ratio of F/A, where F is the force applied to the diamond in kilogram-force and A is the surface area of the resulting indentation in square millimeters as determined by Equations (2) and (3).

$$\mathrm{A} = \frac{\mathrm{d}^2}{1.8544}, \tag{2}$$

where d is the average length of the diagonal left by the indenter in millimeters, hence

$$\mathrm{HV} = \frac{\mathrm{F}}{\mathrm{A}} \cong \frac{1.8544\mathrm{F}}{\mathrm{d}^2}. \tag{3}$$

3. Results and discussion

3.1. Microstructural properties of the samples

The uncoated and coated samples were observed to have polycrystalline morphology. All the coated films were observed to consist of single phase ZnO;. several reflection peaks were observed in the patterns. However, as shown in Figure 2(a), the major element in the stainless steel is Fe and it was observed with a prominent peak found at $2\theta = 74.43°$.

Diffraction peaks for Fe and Ni at 2θ corresponding to Fe and Ni (Ref code: 00-023-0297, FCC crystal structure). Figures 2(b)–(d) show that the coated films are highly crystalline, XRD results (Ref code: 01-079-0208) showed diffraction peaks at an angle 2θ corresponds to ZnO thin films with hexagonal structures.

Ni doping improved the crystallinity of ZnO as presented in Table 2. The position of 2θ for ZnO shifted slightly to a higher angle with Ni doping. This shift is associated with the rearrangement of the microstructure of ZnO with Ni dopant.

The variance in the ionic radii of nickel (0.069 Å) and zinc (0.74 Å) may have resulted to the shift in position of 2θ as Ni content increases. The shift may also result from substitution of Ni ions into Zn ions of the ZnO lattice; similar results are reported by Rajeh *et al* [47]. This shift might also be due to crystal stress in the arrangement because of the addition of Ni atoms to pure ZnO lattice structure. The defects in the crystal structure were formed by the addition of Ni atoms into ZnO lattice and are attributed to the difference in the width and length of the XRD spectra [48, 49]. The average crystal sizes were calculated as 10.66 nm, 11.55 nm,

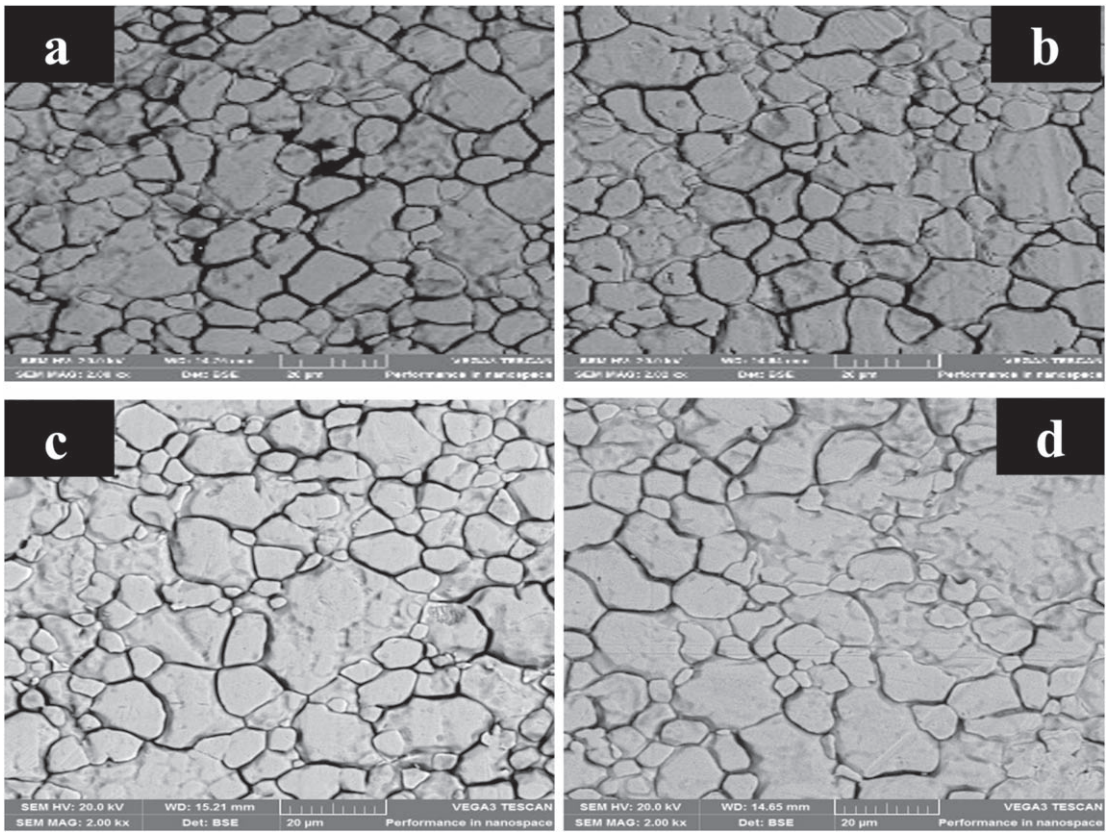

Figure 3. SEM micrographs of (a) S0 (b) S1 (c) S2 and (d) S3.

Table 2. Effect of Ni doping on the microstructure ZnO thin films.

Samples	Pos. ($2\theta^{\circ}$)	Height (cts)	FWHM (°2Th.)	d-spacing (Å)	Av Cryst Size (nm)
S1	35.96	2405.36	0.84	2.50	10.66
S2	35.87	7925.77	0.75	2.50	11.55
S3	36.05	9767.59	0.60	2.49	15.4

and 15.40 nm for 3% Ni-97% ZnO, 6% Ni-94% ZnO, and 9% Ni-91% ZnO thin films respectively. The average crystal size of ZnO was observed to increase with nickel dopant.

3.2. Morphology of the samples

The uniformity and adherence of the deposited films on 316L ST were investigated using SEM. The morphology of the films at the same magnification is shown in Figure 3. The micrographs obtained were used to examine the geometry of the particles.

From the micrographs, the deposited films are crystalline and adhered to the substrates as there was no evidence of spalling, and the films were equally spread across the substrates. The surface of the deposited films showed a surface structure composed of a large irregular shape with little or no observable cracks or pinholes. Surface adhesion and uniformity was reported to have indicated a good growth environment of the deposited nanostructure [50]. The incorporation of Ni^{2+} during growth causes heterogeneous nucleation. The nucleation site number slightly increased as the concentration of Ni^{2+} dopant in ZnO. The propensity for substantial and confined nucleation of grains to occur was reported to be because of degenerate ZnO [51, 52].

3.3. Composition of the samples

The compositions of some selected areas on the SEM micrograph are shown in the EDX characterization shown in Figures 4(a)–(d).

The peaks of the elemental composition of the uncoated and coated samples from EDX characterization are also shown. Table 3 shows the role of Ni doping level on the elemental composition of ZnO films.

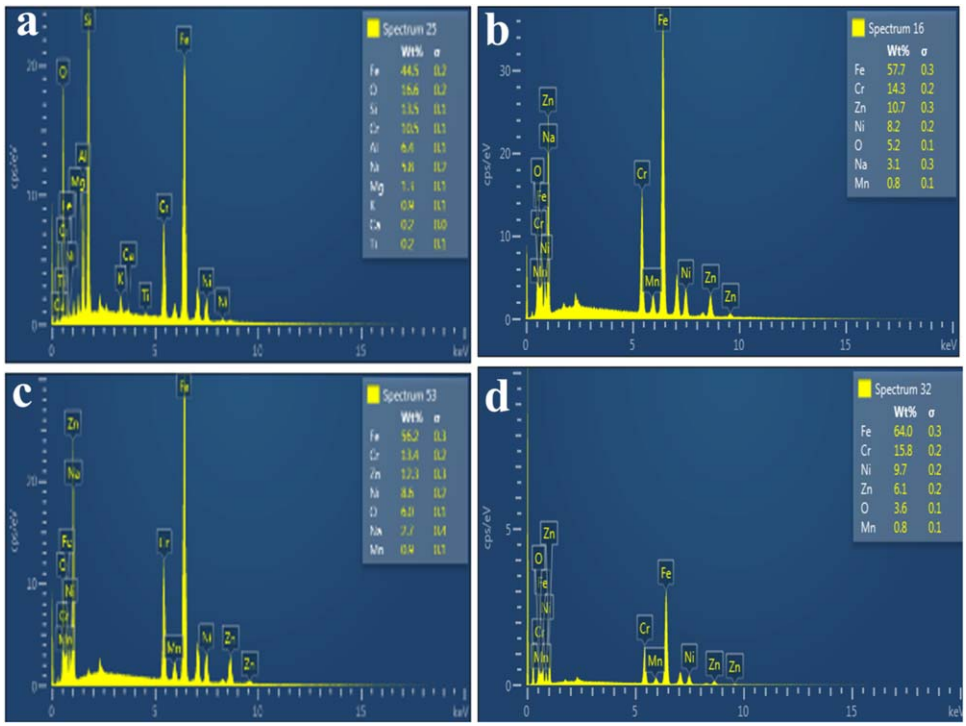

Figure 4. EDX of (a) S0 (b) S1 (c) S2 and (d) S3.

Table 3. Composition of the samples.

Samples	Ni (%))	Zn (%)	O (%)	Fe (%)	Cr (%)	Others (%)
S0	5.80	—	16.60	44.50	10.50	22.60
S1	8.2	10.70	5.20	57.70	14.30	3.90
S2	8.60	12.30	6.00	56.20	13.40	3.50
S3	9.70	6.10	3.60	64.00	15.80	0.80

The major elements in the uncoated 316L ST were found in the proportion of Fe = 44.5%, Cr = 10.5% and Ni = 5.8%, while that of 3%Ni-97%ZnO thin films were determined to be in the proportion of O = 5.2%, Zn = 10.7%, Ni = 8.2%. Also, 6%Ni-94%ZnO were found in the proportion of O = 6%, Zn = 12.3%, Ni = 8.6% and 9%Ni-91%ZnO thin films in proportion of O = 3.6%, Zn = 6.1%, Ni = 9.7% respectively. The EDX results affirmed the presence of O, Ni, and Zn in the deposited samples, this was also confirmed in the XRD spectra. The other elements displayed in the EDX result were observed to be from the 316L stainless steel. The EDX result inveterate the increment in Ni content in the Ni-doped ZnO film. The non-stability of oxygen as Ni content increases in the Ni-doped ZnO film is due to impurities that may have resulted in the structure during deposition. The presence of coated Ni-doped ZnO on the 316L stainless steel covered some signals in the 316L stainless steel matrix.

It is certain that Zn and O are closely bonded from the results obtained, whereas the effect of Ni with O is not easily understood, and probably because Ni is present in the 316L stainless steel. It was observed that as Ni content increases, the % composition of Ni determined in the stainless-steel increases steadily from 8.2 to 9.7 at 9%–91% Ni-doped ZnO at a constant concentration of 0.2 M. Maximum compositions for Zn and O were determined at 6% Ni-doping. The best material would be that obtained at 6% Ni-doping.

3.4. Corrosion properties of the samples

The polarization curves in Figures 5(a)–(e) shows the anodic and cathodic polarization curves for the samples.

At the anode, oxidation reaction usually takes place while the cathodic region is characterized with reduction reaction. The anode region is the active region where corrosion rate is monitored and measured. In this region, the material being subjected to measurement loses electrons to the corrosive environment and is oxidized. Table 4 illustrates the sample's corrosion potential values. The corrosion resistance (corrosion rate) is proportional to the corrosion potential as given by equation (4) [53].

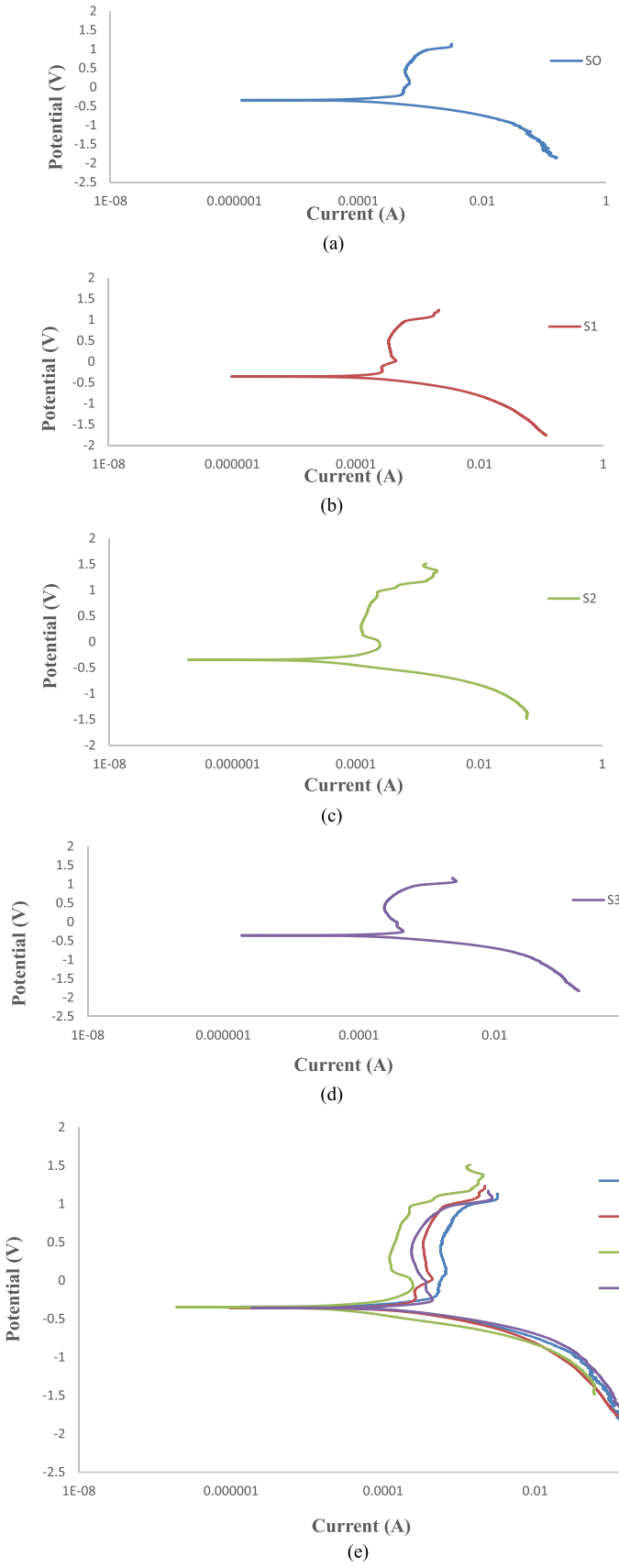

Figure 5. (a)–(e). Anodic and cathodic polarization curves of the samples.

In Figure 5 a comparison of the polarization potential of the uncoated 316L steel to that of coated films was presented. It was also observed that coated 6%Ni-94%ZnO film has the highest polarization potential. The curves were observed to shift towards higher current densities and the working electrode's potential shifted into

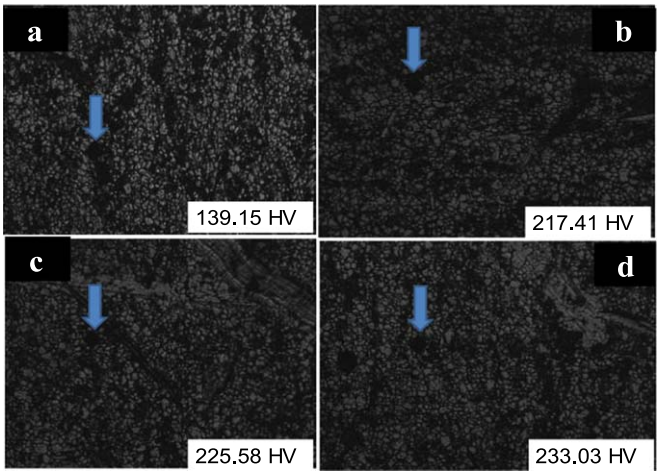

Figure 6. Hardness of the thin films at load 10 g (a) S0 (b) S1 (c) S2 and (d) S3.

Table 4. Samples corrosion potential (CP) and hardness values.

Samples	CP (V)	Hardness (HV)
S0	1.20	139.15
S1	1.30	217.41
S2	1.60	225.58
S3	1.25	233.03

the passive region. The corrosion behavior of the 316L ST was seen to to improve when coated with Ni-doped ZnO films. As observed in Figure 5, it is evident that 6% Ni-94% ZnO reached the maximum polarization potential and is thereby observed to have the best corrosion resistance. It was observed that the sample S2 exhibits a maximum CP value as compared to S3; this may be due to the maximum compositions of Zn that was recorded in sample S2 as reported in Table 3. Zinc has been reported to be the best corrosion protection for steel because it prevents oxygen and moisture from reaching the surface of steel. It also gives cathodic protection at the surface of the steel. The role of Ni in Ni-doped ZnO on the corrosion resistance of the coated stainless steel is shown in Figure 5. The corrosion resistance property of 316L ST improved when it is coated with Ni-doped ZnO thin films. Polarization potential was observed to increase with Ni content and has its maximum value at 6% doping level.

$$R_p = \frac{\partial E_p}{\partial I_p} = \frac{\Delta E_p}{I_p} \tag{4}$$

$$\mathbf{I_p} \rightarrow 0, \quad \mathbf{E_p} \rightarrow \mathbf{E_{corr}}$$

3.5. Hardness properties of the samples

According to Harishanand *et al* [54], hardness is defined as the material's resistance to stress. The Vickers hardness values of the uncoated and coated samples are tabulated in Table 4. Figure 6 shows the samples micrographs being observed under Vickers test. Diamond of load 10 g was used to indent the surface of the films.

The result shows that hardness value of the uncoated 316L ST increases from 139.15 HV to 233.03 HV of 9% Ni-91%ZnO coated film. The hardness value was observed to increase with Ni doping; the increment in the values may have resulted from the rearrangement of grains as Ni content in the films formed a hard phase with the Fe and Cr content in the 316L ST. The increment might also have resulted from the heat treatment resulting from pre-heated 316L ST substrate before deposition. It was observed that Fe and Cr composition changes with Ni content, the significant change in the Fe and Cr composition in the 316L steel may be due to phase that might have been formed between Fe and Ni, Cr and Ni during deposition of films on the stainless-steel substrate.

4. Conclusion

The influence of Ni-doped ZnO thin films on 316L stainless steel was investigated in this paper . It was observed from the SEM result that there is an improvement in the microstructure of the coated samples. The grains in 316L stainless steel are observable in the coated samples S1-S3. This is because of the film's optical transmittance which also confirms that the films are of thin layers in thickness. Samples S1, S2, and S3 show the presence of O, Ni and Zn incorporated into the samples. The other elements displayed in the EDX result are observed to be components of 316L ST. Oxygen content in the sample was observed to decrease from 16.6% of S0 to 3.6% of S3. The corrosion resistance of the 316L ST was observed to improve with the coated Ni-doped ZnO films. The hardness value of the uncoated 316L stainless steel increases from 139.15 HV to 233.03 HV of S3, and the hardness value of the films increases with Ni dopant.

Acknowledgments

The Authors use this medium to appreciate the management of the Center for Energy and Electric Power, Tshwane University of Technology, Pretoria, South Africa for their support towards this research work.

ORCID iDs

Victor Adewale Owoeye https://orcid.org/0000-0002-7544-287X
Ayodeji Olalekan Salau https://orcid.org/0000-0002-6264-9783

References

[1] Shang Y L, Huod L, Ling J Y, Liaoa F H, Ran J L and Xiu L M 2008 Electrorheological property of M-doped (M = Na, Zr) nano-sized TiO_2 particle materials, influence of surface composition and microstructure *Colloids Surf. A: Physicochem Eng. Asp.* **325** 160–5
[2] Krauss G 1992 Advanced surface modification of steels *Journal of Heat Treatment* **9** 81–9
[3] An Y I, Du H Y, Wei Y H, Yang N, Hou L F and Lin W M 2013 Mechanical interfacial structure and properties of surface iron–nickel alloying layer in pure iron fabricated by surface mechanical attrition alloy treatment *Journal of Mater Des.* **46** 627–33
[4] Grum J 2001 A review of the influence of grinding conditions on resulting residual stresses after induction surface hardening and grinding *Journal of Materials Process Technology* **114** 212–26
[5] Visscher H, de Rooji M B, Vroegop P H and Schipper D J 1995 The influence of laser line hardening of carbon steel AISI 1045 on the lubricated wear against steel AISI 52100 *Journal of Wear* **181** 638–47
[6] Baek J M, Cho Y R, Kim D J and Lee K H 2000 Plasma carburizing process for the low distortion of automobile gears *Journal of Surface Coating Technology* **131** 568–73
[7] Shett K, Kumar S and Raghothama P 2009 Effect of ion nitriding on the microstructure and properties of maraging steel (250 Grade) *Journal of Surface Coating Technology* **203** 1530–6
[8] Shi Z and Yan M 1998 The preparation of Al_2O_3–Cu composite by internal oxidation *Journal of Applied Surface Science* **134** 103–6
[9] Stratmann M, Feser R and Leng A 1994 Corrosion protection by organic films *Electrochim. Acta* **39** 1207–14
[10] Grundmeier G, Schmidt W and Stratmann M 2000 Corrosion protection by organic coatings: electrochemical mechanism and novel methods of investigation *Electrochim. Acta* **45** 2515–33
[11] Hagen C H M, Kristoffersen A and Knudsen O O 2016 The effect of surface profile on coating adhesion and corrosion resistance *CORROSION* **15** 2016-7518 https://onepetro.org/NACECORR/proceedings-abstract/CORR16/All-CORR16/NACE-2016-7518/123676
[12] Alvarez R B, Martin H J, Horstemeyer M F, Chandler M Q, Williams N, Wang P T and Ruiz A 2010 Corrosion relationships as a function of time and surface roughness on a structural AE44 magnesium alloy *Corros. Sci.* **52** 1635–48
[13] Hong T and Nagumo M 1997 Effect of surface roughness on early stages of pitting corrosion of Type 301 stainless steel *Corros. Sci.* **39** 1665–72
[14] Zuo Y, Wang H and Xiong J 2002 The aspect ratio of surface grooves and metastable pitting of stainless steel *Corros. Sci.* **44** 25–35
[15] Burstein G and Pistorius P 1995 Surface roughness and the metastable pitting of stainless steel in chloride solutions *Corrosion* **15** 380–5
[16] McBain J W and Hopkins D G 1925 On adhesives and adhesive action *J. Phys. Chem.* **29** 188–204
[17] Brockmann W 1989 Durability of adhesion between metals and polymers *J. Adhes.* **29** 53–61
[18] Hagena C M H, Hognestada A, Knudsenb O O and Sorbya K 2019 The effect of surface roughness on corrosion resistance of machined and epoxy coated steel *Prog. Org. Coat.* **130** 17–23
[19] Ajao J A 2009 Phase transitions in some nickel-rich nickel–boron–titanium hard alloys *Journal of Alloys Compounds* **493** 314–21
[20] Shakoor R A, Kahraman R, Waware U S, Wang Y and Gao W 2014 Synthesis and properties of electrodeposited Ni-B-Zn ternary alloy coatings *International Journal Electrochemical Science* **9** 5520–6
[21] Loto R T 2013 Pitting corrosion evaluation of austenitic stainless-steel type 304 in acid chloride media *Journal of Materials and Environment. Science* **4** 448–59
[22] Fossati A, Borgioli F, Galvanetto E and Bacci T 2006 *Corros. Sci.* **48** 1513
[23] Gouda V K and Hashem A 1992 *Int. Conf. on Advances in Corrosion and Protection, UMIST, UK*
[24] Loto R.T. 2013 Pitting corrosion evaluation of austenitic stainless steel type 304 in acid chloride media *J. Mater. Environ. Sci* **4** 448-459
[25] Wang J H, Su C C and Szklarska-Smialowska Z 1988 *Corrosion* **44** 732
[26] Olejnik L and Rosochowski A 2010 Methods of fabricating metals for nanotechnology, bulletin of the polish academy of sciences *Technical Sciences* **53** 4

[27] Baik S, Estrin Y, Kim H S and Hellmig R J 2003 Dislocation density-based modeling of deformation behavior of aluminum under equal channel angular pressing *Journal of Material Science and Engineering* **35** 86–97
[28] Gonzalez R *et al* 2007 Microstructural study of NiCrBSi coatings obtained by different processes *Journal of Wear* **263** 619–24
[29] Ajao J A 2010 Preparation and structural characterization of vanadium doped Ni-B binary hard alloys, Journal Minerals *Mater. Charact.* **9** 559–68
[30] Otsubo F, Era H and Kishitake K 2009 Structure and phases in Nickel-base self-fluxing alloy coating containing high chromium and boron *Journal Thermal Spray Technology* **9** 107–13
[31] Campbell A N, Mullendore A W, Hills C R and Vandersande J B 1988 The effect of boron on the microstructure and physical properties of chemically vapour deposited Nickel Films *J. Mater. Sci.* **23** 4049–58
[32] Wang Y and Chen W 2004 Microstructures, properties, and high-temperature carburization resistances of HVOF thermal sprayed Ni-Al intermetallic-based alloy coatings *Journal of Surface Coating Technology* **183** 18–28
[33] Chin-You H, Yeh J W, Chen S K and Shun T T 2004 Wear resistance and high-temperature compression strength of FCCCuCoNiCrAl0.5Fe alloy with boron addition *Journal of Metallurgy and Material Transformation* **35A** 1465–70
[34] Knotek O, Lugscheider E and Riemann H 1975 Structure of Ni-rich Ni-Cr-B-Si coating alloy *Journal of Vac Sci Technology* **12** 770–2
[35] Knotek O, Reimann H and Lohage P 1981 Reactions between Ni-Cr-B-Si matrixes and carbide additives in coating duringfusion treatment *Journal of Thin Solid Films* **83** 361–7
[36] Fotovvati B, Namdari N and Dehghanghadikolae A 2019 On coating techniques for surface protection *Journal of Manufacturing and Materials Processing* **28** 1–22
[37] Shajudheen S P M, Saravana K S, Senthil K V, Uma M A, Sivakumar M and Sreedevi R M 2018 Enhancement of anticorrosion properties of stainless steel 304L using nanostructured ZnO thin films *AIMS Mater. Sci.* **5** 932–44
[38] Ibrahim M, Kannan K, Parangusan H, Eldeib S, Shehata O, Ismail M, Zarandah R and Sadasivuni K K 2020 Enhanced corrosion protection of Epoxy/ZnO-NiO nanocomposite coatings on steel *Coatings* **10** 783
[39] Matero R, Ritala M, Leskelä M, Salo T and Aromaa J 1999 Atomic layer deposited thin films for corrosion protection *Journal de Physique IV (Proceedings)* **8** 494–9
[40] Fusco M A, Oldham C J and Parsons G N 2019 Layer deposited Al_2O_3/TiO_2 nanolaminate thin films on copper in 0.1 M NaCl *J. Mater.* **12** 672
[41] Mohamed A, Neto P L, Avaca L A and Aegerter M A 1995 Sol-gel thin films for corrosion protection *Journal of Ceramics International* 403–6
[42] Walter C M 1996 *The International Dictionary of Physics Electronics* (New- York: D. Van Nostrand Company Inc) 1, 124
[43] Owoeye V A, Ajenifuja E, Adeoye E A, Osinkolu G A and Popoola A P I 2019 Microstructural and optical properties of Ni-Doped ZnO thin films prepared by chemical spray pyrolysis technique *Mater. Res. Express* **6** 086455
[44] Adeoye A, Ajenifuja E, Taleatu B A, Ogunmola E D, Omotoso E, Adeyemi O and Babatunde O G 2017 Surface microstructure, optical and electrical properties of spray pyrolyzed PbS and Zn-PbS thin films for optoelectronic applications *J. Mater. Sci.* **35** 576–82
[45] Babalola A V 2017 Effect of concentration and irradiation on the optical and structural properties of ZnO thin films deposited by spray pyrolysis techniques *Journal of Nuclear Inst. and Methods in Physics Research* B **413** 57–61
[46] Kathalingam A, Marimuthu K P, Karuppasamy K, Chae Y, Lee H and Kim P 2019 Structural and mechanical characterization of platinum thin films prepared electrochemically on ITO/glass substrate *Met. Mater. Int.* **10** 20-38
[47] Rajeh S, Barhoumi1 A, Mhamdi A, Leroy G, Duponchel B, Amlouk M and Guermaz S 2016 Structural, morphological, optical and opto-thermal properties of Ni-doped ZnO thin films using spray pyrolysis chemical technique *Journal of Bull. Materials Science* **39** 177–86
[48] Owoeye V A, Ajenifuja E, Babatope B, Osinkolu G A, Popoola A P I and Popoola 0 2019 Experimental investigation and numerical simulation of mechanical properties and thermal stability of tin alloy processed by equal channel angular extrusion (ECAE) *Journal of Engineering Research Express* **1** 025030
[49] Bayram O, Sener E, İgman E and Simsek O 2019 Investigation of structural, morphological and optical properties of Nickel-doped Zinc oxide thin films fabricated by co-sputtering *J. Mater. Sci., Mater. Electron.* **30** 3452–8
[50] Ajenifuja E, Osinkolu G A, Fasasi A Y, Pelemo D A and Obiajunwa E I 2016 Rutherford backscattering spectroscopy and structural analysis of DC reactive magnetron sputtered titanium nitride thin films on glass substrates *J. Mater. Sci.* **27** 335
[51] Kaur G, Mitra A and Yadav K L 2015 Progress in natural science *Journal of Materials International* **25** 12–21
[52] Akinwunmi O O, Ogundeji J A O, Famojuro A T, Akinwumi O A, Ilori O O, Falodun O G and Ajayi E O B 2018 Preparation of some properties of metal organic chemical vapour deposited Al-doped ZnO thin films using single solid precursor *J. Mod. Phys.* **9** 2073–89
[53] Tang L 2002 A study of the polarization techniques for corrosion rate measurement in a steel concrete system *9DBMC* **158** 1–10
[54] Harishanand K S, Nagabhushana H, Nagabhushana B M, Adarsha P, Adarsha A H, Raghavendra M M, Raghavendra N and Vish K R 2013 Corrosion, mechanical and wear properties of nano-zno doped aluminium *International Journal of Engineering Research and Applications* **3** 1569–76